Adaptive Multiple Crossover Genetic Algorithm to Solve Workforce Scheduling and Routing Problem

Haneen Algethami*

College of Computers and Information Technology, Taif University, Saudi Arabia

ASAP Research Group, School of Computer Science, University of Nottingham, UK

Anna Martínez-Gavara*

Estadística y Investigación Operativa, Universidad de Valencia, Spain

Dario Landa-Silva*

ASAP Research Group, School of Computer Science, University of Nottingham, UK

Abstract

The Workforce Scheduling and Routing Problem refers to the assignment of personnel to visits, across various geographical locations. Solving this problem demands tackling numerous scheduling and routing constraints while aiming to minimise the operational cost. One of the main obstacles in designing a genetic algorithm for this problem is selecting the best set of operators that enable better performance in a Genetic Algorithm (GA). This paper presents an adaptive multiple crossover genetic algorithm to tackle the combined setting of scheduling and routing problems. A mix of problem-specific and traditional crossovers are evaluated by using an online learning process to measure the operator's effectiveness. Best performing operators are given high application rates and low rates are given to the worse performing ones. Application rates are dynamically adjusted according to the learning outcomes in a non-stationary environment. Experimental results show that the combined performances of all the operators works better than using one operator in isolation. This study makes a contribution to advance our understanding of how to make effective

*Corresponding author
Email address: hmgethami@tu.edu.sa (Haneen Algethami)

use of crossover operators on this highly-constrained optimisation problem.

Keywords: Genetic algorithms, Adaptive algorithms, Genetic Operators, Routing, Scheduling, Workforce Planning.

1. Introduction

The Workforce Scheduling and Routing Problem (WSRP) is described as the assignment of personnel to visits, requested by customers, across different geographical locations. This problem combines scheduling and routing problems, both of which are known to be NP-Hard [1]. The *scheduling aspect* of the problem assigns personnel to visits in order to fulfil work demands and other requirements. The *routing aspect* of the problem consists of generating routes for the workers to service customers across various locations within given time-windows. The objective is to minimise operational costs while attending the additional requirements expressed by customers, workers and the business. A type of WSRP arises in home health care where nurses and care workers should be assigned to visit patients in their homes in order to carry out some tasks, e.g. administering medication, monitoring serious illness, etc.

Genetic Algorithms (GAs) have been shown to be effective approaches to find solutions for problems combining scheduling and routing where exact methods are less effective, e.g. [2, 3, 4]. A baseline GA was proposed by [5] that identified the best set of operators and parameters for each instance of the same WSRP tackled here. Despite its success in obtaining good solutions, the baseline GA performance was limited by a computationally expensive parameter tuning method. Thus, an adaptive parameter control approach was proposed by [6]. The method maintained diversity in the population of solutions in order to enhance the performance of the GA. On the other hand, in the study by [5], there was no evidence that the performance of one crossover operator was superior to a group of operators during the run. Therefore, a random crossover exchange was proposed by [6] in addition to the parameter tuning method. Further improvements were suggested, especially on operators selection.

This paper proposes an adaptive multiple crossover GA that uses a learning process to enhance the overall performance. The idea is to use to use adaptive allocation rules on a mix of problem-specific and traditional crossovers, which are evaluated to measure the operator's effectiveness. Best performing operators are given high application rates and low rates are given to the worse performing ones. Application rates are dynamically adjusted, to reflect the crossovers behaviour in each iteration, according to the learning outcomes in a non-stationary environment.

This study claims that actively adapting the application rates of a group of crossover operators, can enhance the GA efficiency when tackling WSRP scenarios. To the best of our knowledge, this type of adaptive multiple crossover GA has not been investigated before for WSRP. To this end, the specific objectives of this study are:

- To present an adaptive multiple crossover GA that sets the application rates of several crossovers in a dynamic way.
- To analyse the impact of a collaborative approach between various crossover operators on the quality of solutions as well as on the algorithm speed.
- To carry out illustrative computational tests to show the utility of the proposed GA approach by comparing the performance of the various genetic operators considered. A total of 42 problem instances from six different real-world home health care scenarios were used in the experimental study.

In what follows, Section 2 reviews related work. Section 3 describes the WSRP, its formulation and the instances used in this paper. Section 4 outlines the proposed algorithm. Section 5 presents the experimental study and discusses the obtained results. The paper is then concluded in Section 6.

2. Related Work

Recent research on the WSRP considered here is reviewed next. A mixed integer programming (MIP) with decomposition method [7] required considerable computation time (up to several hours) to solve larger problem instances with hundreds of tasks, indicating the need for faster solution methods. A Variable Neighbourhood Search (VNS) algorithm using problem-specific neighbourhood heuristics was presented in [8]. The VNS obtained high-quality solutions and in less computation time for the same set of problem instances used in [7]. A number of studies have applied GAs to real-world problems where scheduling and routing are combined. Examples include [2, 3]. In those works, the focus has been on algorithm design to obtain good solutions.

An investigation was presented by [4] comparing various genetic operators within two simple GAs, to tackle the subject problem. A more efficient GA was proposed by [5] with tuned parameters and using a customised solution representation to maintain feasibility of solutions. To enhance the GA efficiency, adaptive concepts were used by [6] in addition to random crossover exchange.

Using a learning method, to adjust parameter values has proven to enhance the baseline GA performance [6]. Nevertheless, selecting a random crossover, without any prior knowledge of its performance, was a straightforward procedure. It is still not clear which operator was the best for each problem set, during the run. Thus, this paper proposes a learning-based multiple crossover framework to tackle WSRP.

According to [9], GAs using multiple operators have been used on real-world applications to benefit from the different performance of synchronised operators. Most researchers have utilised a group of operators, crossovers [10] or mutations [11], as part of the algorithm. For example, the study by [12] investigated mixing eight crossover operators on routing problems. One crossover was selected at random, with all the operators having the same probability. This operator is then applied at the current iteration. The study suggested multiple crossovers method obtained better results than a traditional GA. Another study that proposed a multiple operator algorithm for routing problems was presented by [13]. The aim was to test several combinations of operators. The proposed algorithm proved to be more efficient than using one crossover with one mutation.

Two main operations are applied when using multiple operators, **selection** and **evaluation**. Adaptive operator selection (AOS) is identified as the online adjustments of the crossover function [14], where all crossovers are used as one operator. However, each crossover has an application rate, that is relative to the crossover performance. The better the crossover's performance, the higher the chances to be applied more often than a poor performing crossover. This mixes a variety of operator performances in one iteration and the diverse set of operators explore the search space differently and more widely.

Different AOS methods have been successfully used in the literature, including random operator exchange presented in [15, 12, 13]. In later years, adaptive operator allocation rule was developed as a learning-based operator selection function. Such as, probability matching [16], adaptive pursuit [17], multiple armed bandit [18], and sliding multiple armed bandit [19, 20].

In order to measure the effectiveness (performance) of a crossover, an operator evaluation process is used to analyse the impact of applying a given operator on the current search [20]. This method includes giving some reward to an operator according to the operator impact on the search. The next crossover is selected based on a reward value. The best operator is scored higher in the credit registry and therefore this crossover is selected more often.

In general, fitness improvement was used to measure a crossover performance, i.e. the better the new solutions generated by an operator, the more chance of an operator to be applied again. However, more performance measurements were explored and proven to provide good results, such as distance-based measurement [10] and an operator execution-time [9].

Many considerations are taken into account when designing a multiple crossover GA, including the evaluation measurement used and the number of iterations required to obtain sufficient information on the operators' performance. Existing research has focused on using a fixed number of iterations to determine "the best" operator. However, an AOS might converge to the best performing operator early in the search. Not to mention that different operators provide different results at different stages of the search. Thus, using preliminary information can have limited flexibility and leads up to a loss of performance. This observation was proved by [14], in which the use of a "dynamic" approach was shown to be better than using a "static" one.

The GA proposed here uses allocation rules on a mix of problem-specific and traditional crossovers. Best performing operators are given higher application rates, and lower rates are given to the worse performing operators. Application rates are dynamically modified during the search using a roulette wheel [16, 17]. This paper shows that adaptive application rates enhance the GA efficiency when tackling WSRP scenarios.

3. Problem Description

A WSRP solution S is a daily plan of visits, i.e. a set of workers W assigned to perform a set of tasks T for customers at different locations. The assignment of a worker w to travel to a customer location in order to perform a task $i \in T$ is called a visit. Several features have been identified as important in solutions to WSRP scenarios, such as distance travelled and customers' and workers' requirements and preferences [21]. Thus, a good quality solution should have low operational cost as well as all visits assigned while satisfying the existing requirements. For example, an illustration of a plan for a WSRP instance is presented in Fig. 1. In this example, 3 workers (w_1, w_2, w_3) are assigned to 15 different visits, located at different locations. A path is plotted as a dotted line with a different colour for each worker. Each worker is assigned a set of visits, note visits 5 and 9 require two workers.

3.1. Problem Constraints

Table 1 lists the objectives and constraints in the WSRP considered here as described in [7]. The binary decision variable $x^w_{i,j} = 1$ if worker w travels from visit i to visit j, thus w is assigned to both visits as given by constraint (1).

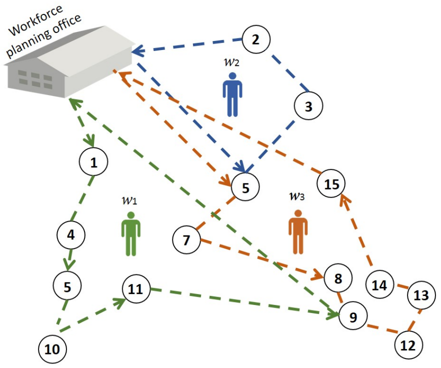

Fig. 1: Example of a WSRP solution with 3 workers and 15 visit assignments.

Table 1: Objectives and Constraints in the WSRP.

Objectives	**Hard constraints**	**Soft constraints**
Minimise the Travelling cost	Assign all visits. eq.(2)	Respect workers area availability. eq. (13)
Minimise the Payment cost	Respect visit time (No time-conflicts). eq.(9)	Respect workers time availability. eq.(10,11).
Minimise Penalty cost	Respect max working time per week. eq.(12)	Assign preferred workers to visits
	Assign qualified workforce. eq.(7)	Assign preferred workers with a specific skill
		Assign workers to preferred areas

$$\sum_{i\in T}\sum_{j\in T} x_{i,j}^{w} = \sum_{n\in T} x_{j,n}^{w}, \forall w \in W \tag{1}$$

In WSRP scenarios, it is possible that some visits are left unassigned if there is not enough workforce or no worker has the required qualifications/skills 145 for some visits. In such cases, an integer variable y_j is used to indicate the number of unsatisfied assignments for visit j (the visit may require more than one worker) [7, 22].

If visit j is fully assigned then $y_j = 0$, otherwise y_j takes a positive integer value equal to the number of workers required to the visit. Constraint (2) 150 ensures this requirement is met even for visits that are unassigned, r_j is the number of workers required for visit j.

$$\sum_{w\in W}\sum_{i\in T}\sum_{j\in T} x_{i,j}^{w} + y_j = r_j \tag{2}$$

The path for each worker w should begin at a start location and terminate at an end location, e.g. their home or a central office. The start location and the end location of worker w are D_w and D'_w, respectively. The condition is enforced by constraints (3) and (4). Workers may leave their start location and enter their end location at most once (although the start and end locations may be different) as expressed by constraints (5) and (6), respectively.

$$\sum_{n \in T} x^w_{n,j} \geq \sum_{j \in T} x^w_{i,j}, \forall w \in W, \forall i \in T, \exists n \in D \tag{3}$$

$$\sum_{n \in T} x^w_{i,n} \geq \sum_{i \in T} x^w_{i,j}, \forall w \in W, \forall j \in T, \exists n \in D' \tag{4}$$

$$\sum_{j \in T} x^w_{i,j} \leq 1, \forall w \in W, \forall i \in D \tag{5}$$

$$\sum_{j \in T} x^w_{i,j} \leq 1, \forall w \in W, \forall j \in D' \tag{6}$$

Workers are required to have suitable skills for every assigned visit. Let q^w_j be a binary parameter that represents some qualification parameter, where q^w_j $= 1$ when a worker w has the skills to take visit j, and $q^w_j = 0$ otherwise. Only qualified workers can make the visit as indicated by constraint (7).

$$x^w_{i,j} \leq q^w_j, \forall w \in W, \forall i \in T, \forall j \in T \tag{7}$$

Travelling between visit locations must be feasible in terms of travel time. Decision variable a^w_j takes a positive fractional value that gives the arrival time of worker w to the location of visit j. Note that the maximum arrival time value here is 1440 minutes, which is equivalent to the 24^{th} hour of the day. Let a^w_i, a^w_j be the arrival times of worker w at the locations of visit i and visit j respectively. The arrival time at visit j must consider the time duration δ_i spent on performing visit i and the travelling time $t_{i,j}$ between visit i and visit j. This is enforced by constraint (8) where M is a large constant number.

$$a^w_j + M(1 - x^w_{i,j}) \geq a^w_i + x^w_{i,j} t_{i,j} + \delta_i, \forall w \in W, \forall i \in T, \forall j \in T \tag{8}$$

A worker w must arrive at visit j within the given time-window. For visit j, the earliest arrival time is κ_j^L and the latest arrival time is κ_j^U. This requirement is enforced by constraint (9).

$$\kappa_j^L \leq a_j^w \leq \kappa_j^U, \forall j \in T, \forall w \in W \tag{9}$$

If a visit j assignment has time conflicts with the visit i assignment, $\tau_j^w = 1$. A time-conflict occurs when a worker is assigned to visits overlapping in time.

Time availability can be different for each worker according to their individual contracts. The time availability period for each worker is as follows. The shift start-time and shift-end time of the worker w are indicated by α_L^w and α_U^w respectively. However, in the scenarios tackled in here, visits can be assigned outside the worker's shift but subject to a penalty cost. A binary decision variable $\omega_j^w = 1$ is introduced to indicate such penalisation. The time availability constraints for worker w are given by expressions (10) and (11).

$$\alpha_L^w - a_j^w \leq M(1 - x_{i,j}^w + \theta_j^w), \forall w \in W, \forall i \in D \cup T, \forall j \in T \tag{10}$$

$$a_j^w + \delta_j - \alpha_U^w \leq M(1 - x_{i,j}^w + \theta_j^w), \forall w \in W, \forall i \in D \cup T, \forall j \in T \tag{11}$$

Another working regulation tackled here is not to exceed the maximum working hours for each worker. Each visit j requires δ_j minutes to be completed. The maximum working hours for a worker w is given by h^w. Constraint (12) enforces this regulation.

$$\sum_{i \in V^S} \sum_{j \in T} x_{i,j}^w \delta_j \leq h^w, \forall w \in W \tag{12}$$

Each worker is associated to a set of geographical regions defined by the service provider. A geographical region contains several visit locations and a visit location may have several visits to be assigned. Ideally, a worker should only be assigned to visits in those geographical regions. However, if necessary, a worker can be asked to travel to locations outside their geographical regions subject to some penalty cost. A binary parameter $\gamma_j^w = 1$ is defined to indicate that visit j is located in the worker's regions and $\gamma_j^w = 0$ otherwise. A binary variable $\psi_j^w = 1$ to indicate that visit j assigned to worker w is outside the worker's regions, and $\psi_j^w = 0$ otherwise. Constraint (13) presents the relation between these binary variables for the different possible cases.

$$\sum_{i \in T} x_{i,j}^w - \psi_j^w \leq \gamma_j^w, \forall w \in W, \forall j \in T \tag{13}$$

Some of the constraints expressed in the above MIP formulation are soft constraints in WSRP scenarios, including constraints (10) and (11) (workers may be asked to work outside their shift hours) and constraint (13) (workers may be asked to work outside their geographical regions). Later, preferences calculations are explained as they are used as part of the objective function.

3.2. Objective Function

The objective function includes the *operational cost* and the *penalty cost.* The operational cost includes wages plus journey costs for all workers and is given by the accumulated cost $d_{i,j} + p_j^w$, where $d_{i,j}$ is the distance travelled between visit i to visit j and p_j^w is the cost of assigning worker w to visit j. These costs are set by the service provider in the HHC scenarios used here.

Since feasibility is not guaranteed in a WSRP solution, the penalty costs are tackled as the accumulated penalty for violations of the constraints presented in Table 1.

An assignment of worker w to visit j is made to a path connecting between two nodes and can be written as a tuple $\left(x_{i,j}^w, y_j, a_j^w, \psi_j^w, \theta_j^w, \tau_j^w\right)$. This assignment is composed of binary decision variables indicating violations occurrences on area availability (ψ_j^w), time availability (θ_j^w) and conflicting assignments (τ_j^w). If a visit j violates time availability, then $\theta_j^w = 1$. The same applies to area availability violation where $\psi_j^w = 1$, when violation occurs. Likewise, τ_j^w $= 1$, if the assignment has time conflicts with the other assignment.

The non-satisfaction of preferences is also included in the penalty cost. There are three types of preferences including preferred worker-customer pairing, worker's preferred region and customer's preferred skills. There is a degree of satisfaction for these preferences when assigning a worker w to a visit j and is given by ρ_j^w which has a value that ranges between $\big[0, 3\big]$, where 0 means no penalty charged and 3 is full penalty.

For each assignment, the satisfaction value for each preference ranges between $\big[0, 1\big]$, from not satisfied to satisfied. There are four-level preferences: low (0.2), neutral (0.5), preferred (0.5), and most preferred (1.0). The satisfaction level is calculated by reverting it to a penalty, by subtracting it from the full satisfaction score, which is $3r_j$ for a visit j.

The best solution should have: the least *operational cost* and the least *penalty cost*. A weighted sum is proposed to combine the objectives into a single scalar value [8, 5]. The objective function is written as in equation (14), where weights $\lambda_1, \ldots, \lambda_5$ are defined to establish priority between objectives (more about the weights used here next).

$$\begin{aligned} f(S) = \lambda_1 \sum_{w \in W} \sum_{i \in T} \sum_{j \in T} (d_{i,j} + p_j^w) x_{i,j}^w, \quad & \textit{operational cost} \\ + \lambda_2 \sum_{w \in W} \sum_{i \in T} \sum_{j \in T} (3r_j - \rho_j^w) x_{i,j}^w & \\ + \lambda_3 \sum_{w \in W} \sum_{j \in T} (\psi_j^w + \theta_j^w) + \lambda_4 \sum_{j \in T} y_j + \lambda_5 \sum_{w \in W} \sum_{j \in T} \tau_j^w, \quad & \textit{penalty cost} \end{aligned} \tag{14}$$

3.3. Weights Calculation

Table 2: Weights values for WSRP

Objective	Operational costs	Preferences penalty costs	Soft constraints penalty	Unassigned visits	Time-conflicts
Weight	λ_1	λ_2	λ_3	λ_4	λ_5
Value	$mileage/k$	1	$\frac{\lvert V \rvert}{2}$	${\lambda_3}^2$	${\lambda_3}^3$

The weights associated with each objective are set to values that reflect the difference between the priority levels, as suggested by [22, 23]. The main goal is to maintain a balance of priorities for each instance based on each problem specifications. Thus, the weights calculations presented in Table 2 differ from one instance to another [1].

Hard constraint violations are not allowed in the WSRP solution.However, time conflicts constraint is more difficult to satisfy. Thus, the highest priority level is given to minimise the conflicting assignments τ_j^w, where the associated weight λ_5 is set to the highest value. In this work, a solution with conflicting assignments is an infeasible solution.

The second highest priority to be minimised is the unassigned visits y_j where λ_4 is set to be very high, but still less than the value of λ_5. This is due to the service provider requirements for completing as many visits as possible. However, in this study, a chromosome representation ensures all visits to be assigned to workers, hence no unassigned visits violations. This is explained later in the next chapter.

In practice, the service provider may ask workers to undertake visits that are outside their time availability and/or geographical region. Thus, the next objective priority is λ_3, given to minimise the soft constraints penalty, i.e., the number of workers with time-availability violations ψ_j^w and the number of workers with area-availability violations θ_j^w. As presented by Table 2, the weight values for λ_3, λ_4 and λ_5 are relative to the number of the assigned visits, therefore only assigned visits are violated. On the other hand, if the service provider could not fulfil the highest preference level; the fourth priority is given to minimise the preferences penalty through λ_2.

Finally, the lowest priority is given to minimise the operational cost through λ_1. This weight value is presented in Table 2, where k is the operational cost. Hence, mileage is calculated for the assigned workers only.

Hard constraint violations are always penalised with a larger weight than soft constraints. Accordingly, $\lambda_3 + \lambda_4 + \lambda_5 > 1$ while $\lambda_1 < 1$. Under those conditions, the objective is shifted to minimise the constraint violations, by

[1] The weights used here are available as "Evaluation Tool" (blue setting) at `https://goo.gl/1733qY`

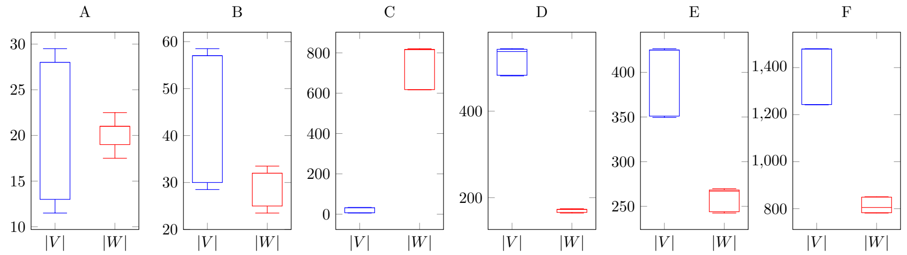

Fig. 2: Box plots comparisons of WSRP scenarios dimensions, shown as the number of visit assignments V and the number of workers W.

moving the $f(S)$ cost-value closer to the feasible region.

3.4. Problem Instances

Table 3: Main Features of the 42 Home Health Care Problem Instances.

	A								B							
	01	**02**	**03**	**04**	**05**	**06**	**07**	**mean**	**01**	**02**	**03**	**04**	**05**	**06**	**07**	**mean**
Number of Visits	31	31	38	28	13	28	13	26	36	12	69	30	61	57	61	46
Number of Workers	23	22	22	19	19	21	21	21	25	25	34	34	32	32	32	30
Number of Areas	6	4	5	4	4	8	4	5	6	5	7	5	8	8	7	7

	C								D							
	01	**02**	**03**	**04**	**05**	**06**	**07**	**mean**	**01**	**02**	**03**	**04**	**05**	**06**	**07**	**mean**
Number of Visits	177	7	150	32	29	158	6	80	483	454	585	520	538	610	611	543
Number of Workers	1037	618	1077	979	821	816	349	813	164	166	174	174	173	174	173	171
Number of Areas	8	4	7	8	6	11	6	7	13	12	15	15	15	15	15	14

	E								F							
	01	**02**	**03**	**04**	**05**	**06**	**07**	**mean**	**01**	**02**	**03**	**04**	**05**	**06**	**07**	**mean**
Number of Visits	418	425	462	351	461	301	498	416	1211	1243	1479	1448	1599	1582	1726	1470
Number of Workers	243	244	267	266	278	278	302	268	805	769	898	789	889	783	1011	901
Number of Areas	13	14	15	13	15	13	16	14	45	46	54	47	59	44	64	51

Problem instances from six UK real-world Home Health Care (HHC) scenarios are used as instances of WSRP in this study [2]. There are 7 problem instances in each scenario for a total of 42 instances. Table 3 shows the main features of each problem instance. Scenario A instances are considered the smallest, while instances in scenario F are the largest. Problem instances in scenario C are of disproportional nature as the number of workers is much larger than the number of visits.

[2] The instances used here (A, B, C, D, E and F) are available at `https://goo.gl/1733qY`

Fig. 2 shows a group of box plots for each WSRP problem set comparing the total number of visits $|V|$ and the total number of workers $|W|$. The difference between the number of visits and the number of workers increases through the problem sets. In some, the number of visits is larger than the number of workers available. However, in problem set C, the number of visits is less than the number of workers.

Table 4: Cost-values $f(S)$ and computational-time Cpt (in seconds) for WSRP instances produced by the MIP solver in [7].

Problem		$f(S)$	Cpt	**Problem**		$f(S)$	Cpt	**Problem**		$f(S)$	Cpt
A	**1**	3.49	7	**C**	**1**	n/a	n/a	**E**	**1**	n/a	n/a
	2	2.49	8		**2**	3.15	6		**2**	n/a	n/a
	3	3	14		**3**	n/a	n/a		**3**	n/a	n/a
	4	1.42	5		**4**	11.15	90		**4**	n/a	n/a
	5	2.42	1		**5**	12.34	55		**5**	n/a	n/a
	6	3.55	5		**6**	n/a	n/a		**6**	n/a	n/a
	7	3.71	1		**7**	4.3	1		**7**	n/a	n/a
B	**1**	1.7	21	**D**	**1**	n/a	n/a	**F**	**1**	n/a	n/a
	2	1.75	2		**2**	n/a	n/a		**2**	n/a	n/a
	3	1.72	6003		**3**	n/a	n/a		**3**	n/a	n/a
	4	2.07	25		**4**	n/a	n/a		**4**	n/a	n/a
	5	1.82	585		**5**	n/a	n/a		**5**	n/a	n/a
	6	1.62	184		**6**	n/a	n/a		**6**	n/a	n/a
	7	1.79	300		**7**	n/a	n/a		**7**	n/a	n/a

Table 4 presents optimal results by a mixed integer programming (MIP) solver in [7]. Researchers have reported that real-world instances of the WSRP are difficult to solve [24, 23]. This was also observed [7] where the MIP solver was unable to provide solutions for 24 instances, shown as *n/a*) in Table 4.

4. Adaptive Multiple-Crossover Genetic Algorithm (AMCAGA)

This section describes the proposed adaptive mechanisms of the AMCAGA as an extension of the GA approach in [5] and the diversity-based adaptive GA (AGA) in [6] which was shown to provide best results in comparison to other adaptive variations implemented for WSRPs. Algorithm 1 shows the steps of this proposed algorithm.

Algorithm 1 Adaptive Multiple-Crossover Genetic Algorithm (AMCAGA)

```
Require: A crossover rate $P_c$, a mutation rate $P_m$, set of crossovers $\chi = x_1, x_2 \dots x_L$, $WSL$ for all visits.
 1: Create a population $P$ of $M$ individuals using $WSL$
 2: repeat
 3:     Evaluate each individual in $P$ with equation (14)
 4:     for $9M/20$ times do
 5:         Select $p_1, p_2 \leftarrow P$
 6:     end for
 7:     Select $x_i \leftarrow \chi$ with $P_{x_i}$
 8:     $(o_1, o_2) \leftarrow x_i(p_1, p_2)$ with $P_c$, for all pairs of parents
 9:     $Score_i \leftarrow$ Performance of $x_i$
10:     Update $P_{x_i} \leftarrow Score_i / Score_{Sum}$
11:     $(o_1', o_2') \leftarrow FCF(o_1, o_2)$ with $P_m$, for all pairs of offspring
12:     $(o_1', o_2') \rightarrow P'$, for all pairs of offspring
13:     $P$ best $M/10$ individuals $\rightarrow P'$
14:     if $P$ has stagnated for a number of generations then
15:         if $P_c > 0.45$ AND $P_c < 1.0$ then
16:             Update $P_c$ according to equation (15)
17:         else
18:             Reset $P_c$
19:         end if
20:         if $P_m > 0.1$ AND $P_m < 0.60$ then
21:             Update $P_m$ according to equation (16)
22:         else
23:             Reset $P_m$
24:         end if
25:     end if
26:     $P' \rightarrow P$
27: until termination condition is met
```

The proposed AMCAGA works as follows. First, an initial population P of M individuals (one-day plans) is created based on an indirect chromosome encoding (worker suitability list or WSL) to ensure solutions feasibility (line 1). At the start of each generation, $9M/20$ pairs of parent individuals are selected using binary tournaments (lines 4–6). With some probability P_{x_i}, a crossover x_i is selected, using roulette wheel selection (line 7). This crossover, with some probability P_c, is applied to each pair of parents to generate two offspring (line 8). The operator' performance is evaluated and recorded (lines 9–10). With some probability P_m, each offspring goes through a flat-cost flip (FCF) mutation operator (line 11). These offspring are added to the new population P'

(line 12). An elitism strategy keeps the $M/10$ best individuals from the current population P. Along with the $9M/20$ offspring individuals generated, the new population P' of M solutions is formed (line 13). If there are no cost value improvements on the best-so-far solutions for a number of generations, the GA is considered to have stagnated. Thus, P_c and P_m are modified at every generation, depending on the results obtained in the previous one, to maintain a diverse population and therefore improve the effectiveness of the search (lines 14–25). The indirect chromosome encoding, genetic operators, adaptive parameter updates and multiple crossover mechanism are described next.

4.1. Indirect Chromosome Encoding

According to [13], the crossover process is not efficient for the optimisation capacity of the technique when it is applied to routing problems using path encoding. Thus, an indirect chromosome encoding scheme was proposed in our earlier study [5]. The aim is to construct feasible solutions by considering suitable workers only. To do so, a *worker suitability list (WSL)* is created for each visit v_i. Suitable workers are ranked by a penalty score, the lower the score value, the better suited is a worker. The score estimates the impact of assigning worker w_j to visit v_i, considering incurred operational cost and penalty cost due to preferences and availability restrictions.

An solution is randomly created by generating a vector of $|V|$ integers between 0 and $L_k - 1$, where V is the number of visits and L_k is the length of WSL for a visit k. When a worker is being considered for a visit, the solution is evaluated for time-conflicts. If such conflict occurs by the random assignment, the next worker in the WSL for that visit is considered until a suitable worker is found with no time-conflicts arising.

Fig. 3 illustrates an example of the indirect chromosome encoding for a day plan with seven visits. Each visit has a WSL of four suitable workers, with the best worker for that visit at the top, followed by the next best worker and so on. Below the chromosome, the decoded solution shows the actual worker assigned to each visit. On the right, the encoded solution is shown with an index of the workers as in the WSL for each visit. Time-conflicts are indicated with *.

For example, w_2 is assigned to both v_1 and v_3 while w_3 is assigned to v_2. No time-conflict arises because v_1 and v_3 do not overlap. However, w_2 is assigned to v_4 and a time-conflict arise as v_3 overlaps with v_4. Then, the next most suitable worker that does not provoke a time-conflict, in this case w_5, is assigned to v_4. The WSL decoder in this indirect chromosome encoding scheme helps to assign suitable workers to visits while avoiding time-conflicts. The penalty scores are shown in Fig. 3 are not used during the generation of initial solutions, they are utilised for the tailored genetic operators described in [5]. Note that the indirect chromosome representation is designed to include all assigned visits $|V|$, thus the chromosome length varies according to the problem-size.

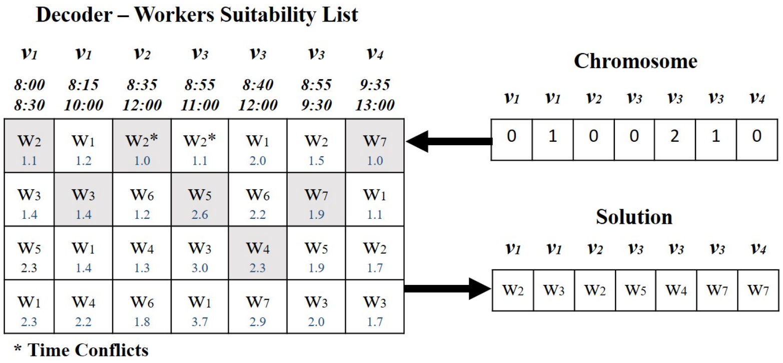
Decoder – Workers Suitability List
v1 v1 v2 v3 v3 v3 v4
8:00 8:30
8:15 10:00
8:35 12:00
8:55 11:00
8:40 12:00
8:55 9:30
9:35 13:00
0: W2 1.1 | W1 1.2 | W2* 1.0 | W2* 1.1 | W1 2.0 | W2 1.5 | W7 1.0
1: W3 1.4 | W3 1.4 | W6 1.2 | W5 2.6 | W6 2.2 | W7 1.9 | W1 1.1
2: W5 2.3 | W1 1.4 | W4 1.3 | W3 3.0 | W4 2.3 | W5 1.9 | W2 1.7
3: W1 2.3 | W4 2.2 | W6 1.8 | W1 3.7 | W7 2.9 | W3 2.0 | W3 1.7
* Time Conflicts
Chromosome
v1 v1 v2 v3 v3 v3 v4
0 1 0 0 2 1 0
Solution
v1 v1 v2 v3 v3 v3 v4
W2 W3 W2 W5 W4 W7 W7

Fig. 3: An example of indirect chromosome encoding scheme for illustration.

4.2. Genetic Operators

The AMCAGA incorporates various genetic operators including some problem-specific ones that utilise heuristics to generate improved offspring [5]. All operators used are taken from [5]. A mix of general purpose and problem-specific operators are used. The general purpose ones are one-point crossover (1PX) [25], two-point crossover (2PX) [25], uniform crossover (UX) [25] and half uniform crossover (HX) [25]. Three problem-specific operators are considered, specially designed for the solution representation considered here. These are flat-costs crossover (FCX) [5], partially-matched flat crossover (PMFCX) and flat-cost flip mutation (FCF) [5]. These operators are described below.

1. **1PX:** A point between 1 and the chromosome length is selected at random. To create one offspring, the genes before this point are copied from one parent and the genes after are copied from the other parent. Another offspring is created using the other half from each parent.
2. **2PX:** Two points are selected at random, between one and the chromosome length. Alternating segments are swapped to create the two offspring.
3. **UX:** The number of crossing points is not fixed. Instead, a mixing ratio (50%) is used to choose a uniform random real number u from interval $< 0, 1 >$ when mixing the parents to create the offspring. Individual non-matching genes are swapped between the two parents with the given mixed ratio to create the offspring [26].
4. HX: Similar to UX, a mixing ratio is used. However, exactly half of the non-matching genes are swapped. Thus, the Hamming distance (number of differing gens between the two parents) is calculated and divided by two.
5. **FCX:** Uses penalty scores that were initially calculated in the WSL at the start of the GA. These values are denoted as 'flat-cost', where each worker w_j has a penalty score according to their suitability to work in visit i. FCX goes through each of the V positions in the parent's chromosome. A gene-wise comparison is enforced, for each gene in i^{th} position, with respect to the WSL estimated penalty scores M_{i,p^i}. The best suitable worker is given to offspring (o_1) and the other worker for offspring (o_2).
6. **PMFCX:** This crossover selects a segment within two cutting points. Positions of genes are reversed between these points and the FCX is applied to fill the rest of the offspring.
7. **FCF:** Introduces new workers to the chromosome, even if the workers are not suitable for the corresponding visits. A random position i of

the chromosome is replaced. Hence, FCF increases the diversity by the random process, even if the best worker for visit i is not selected. $p_i = (0, 1, 0, 0, 2, 1, 0)$. If positions 3 is selected at random, gene 0 is replaced by a random number within the list of visit i in WSL, to generate the child chromosome $o_j = (0, 1, 3, 0, 2, 1, 0)$.

4.3. Adaptive Parameter Rates

Initial parameter values, P_c and P_m, were selected after an offline tuning method [5]. Then, P_c and P_m are modified at every generation and to avoid early convergence, a diversity-based scale is used to calculate the required change in the adaptive features. Population diversity is measured in two ways as described below. The two measurements accommodate different views of the loss of diversity. Combining these methods can overcome those difficulties faced by one measurement used in isolation [27].

- *The genotype space* [28], denoted as $Diversity_g$. It is the distribution of pairwise differences between individuals in a population.
- *The phenotype space*, denoted as $Diversity_p$. It is the population fitness variance, i.e., how far each individual in the population is from the mean fitness value.

Population diversity has an effect on the setting of parameter values [6]. For example, if instances are relatively small, a large population size M is required as a result of the large degree of similarity between individuals in P. When similar individuals are recombined, inbreeding occurs, and no additional diversity is added through crossover. For a large instance, there is less chance to have similar solutions, thus, a small M is sufficient.

Whenever the best solution found by the technique has not been improved in the last generation, rates are updated, according to the calculations in [6]. This means that the search process did not evolve correctly and that it is necessary to diversify the population through adaptive parameter rates.

Equation (15) calculates the updates on P_c value, where Q_1= 45% and Q_2= 100%. Equation (16) calculates the updates on P_m value, where Q_1= 10%.

$$P_c = \left[\frac{Diversity_g}{Diversity_p} * (Q_2 - Q_1)\right] + Q_1 \tag{15}$$

$$P_m = \frac{\frac{Diversity_p - Diversity_g}{Diversity_p} \times Q_1 + \frac{f(S)_{max} - f(S)}{f(S)_{max} - f(S)_{min}} \times Q_1}{2} \tag{16}$$

A resetting process is also used to reset $P_c = 45\%$ and $P_m = 10\%$ to forget the rates history if the rates values are out of range. This means forgetting all the previous feedback process that led up to the inflation of the adapted values. More details of the AGA framework is described in [6].

4.4. Adaptive Multiple Crossover Framework

The proposed AMCAGA uses a set of crossovers $\chi = x_1, x_2 \ldots x_L$, which are alternated during the execution, similar to [13]. However, the strategy used in this paper uses allocation rules rather than random replacement.

At the beginning, a number of the crossover functions are applied, until the next generation is created. This number is indicated as the memory size σ. One operator is assigned at random and then replaced by another crossover. All crossovers are applied uniformly, to ensure all crossovers are used, while allowing repetitions. There is at least $\frac{1}{L}$ chance for each operator to be selected.

The operators' performances are evaluated and recorded as *scores* for a number of iterations during the learning process (also denoted as a cycle of a size v). For each crossover, the accumulated scores are stored into the **crossover reward matrix (CRM)**, considered as a reward registry for that crossover in the current cycle. Scores are then transformed into **application rates** P_{x_i}, giving the probability of applying crossover x_i. The operators' performances are evaluated and recorded for each cycle, where application rates are dynamically adjusted as the search progress.

Better performing operators have a higher score value, and therefore a higher probability to be utilised more often, but weak performing operators are not left without a chance. For example, given a set χ of six crossovers operators, with application rates as follows: $x_1 = 23$ %, $x_2 = 4$ %, $x_3 = 11$ %, $x_4 = 34$ %, $x_5 = 17$ % and $x_6 = 12$ %. Crossover x_4 has the highest application rate at this cycle, henceforth x_4 has more chance to be implemented. At some point of the search, when x_4 performance changes for the worse, its application rate decreases. Application rates of other crossovers also vary accordingly, causing a shift in the search.

4.4.1. Performance Measurements

Scores are considered as performance indicators that enforce the rewarding mechanism, $\forall x_i \in \chi$, a score is given at each iteration, where $i = 1, 2 \ldots, L$. Different types of measurements are used in the literature, such as fitness-based measurement [29, 20], distance-based measurement [10] and combined measurement and operator execution-time measurement [9]. In this study, the later can be relative to the problem size for WSRPs. Hence, the time is not absolute in real-world settings, and therefore this measurement is excluded.

Parameter settings are affected by the population diversity [6]. Therefore, distance-based measurement is considered here along with the fitness-based measurement. Performance measurements used in this chapter are as follows.

- **Fitness-Based**. This method is selected to maximise the cumulative improvement, as a historical fitness record of the cost value of an offspring (o) and its parent (p), where $f(o) < f(p)$. When there is an improvement on the overall cost value, the score increases by one. This value ensures the convergence by selecting crossovers with better offspring quality, that eventually improves the overall performance of the GA.

- **Distance-Based**. This method is selected to ensure a level of diversity among generated solutions, by calculating the distribution of the pairwise differences between an offspring and its parent. If the percentage is 60% or more, the score increases with respect to the *hamming distance* H between two individuals. This value is selected to prevent inbreeding among generations. The value of H is calculated as the number of assignments in which the corresponding genes are different. Fig. 4 illustrates an example of the dissimilarities percentage calculations (presented in white cells) between a parent and an offspring.

- **Hybrid Approach**. This method is selected to harness the power of the two above measurements. When there is an improvement in the fitness or there exist differences between parents and offspring, the score increases. This means that with every crossover evaluation, the score value increases gradually. If only one measurement has proved an operator efficiency, the score value increases by one. On the other hand, if both performance measurements have proved an operator efficiency simultaneously, the score value increases by two.

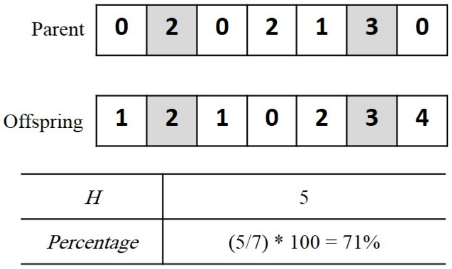

Parent	0	2	0	2	1	3	0
Offspring	1	2	1	0	2	3	4

H	5
Percentage	(5/7) * 100 = 71%

Fig. 4: An illustration of the dissimilarities percentage (presented in white cells) between two individuals (parent, offspring).

Each crossover is evaluated in isolation with a performance measurement after each application. Details of the application rates calculations are given next.

4.4.2. Application Rates

At each iteration (cycle), one of three above mentioned performance measurements (fitness, distance or hybrid) evaluate all crossovers, and then gives a score value $\forall x_i \in \chi$, where $i = 1, 2 \ldots, L$. For the next iteration, scores are updated, until all cycles are completed. The accumulated score value over different cycles is then transformed to an application rate $P_{x_i} = \frac{Score_i}{Score_{Sum}}$, where $Score_{Sum} = \sum_{i=1}^{L} Score_i$.

When recording the accumulated scores, a $2 \times L$ matrix is used, noted as crossover rewards matrix (CRM), i.e. the score value in $(1, i)$ is added to the value in $(2, i)$. The $2 \times L$ CRM is used to allow faster computation. As a result of scores updates, a gradual change in the P_{x_i} value is recorded in CRM, with no rapid increase or decrease in the overall application rates. This process is repeated, for each cycle. Note that the application rates are always modified before the next cycle (iteration).

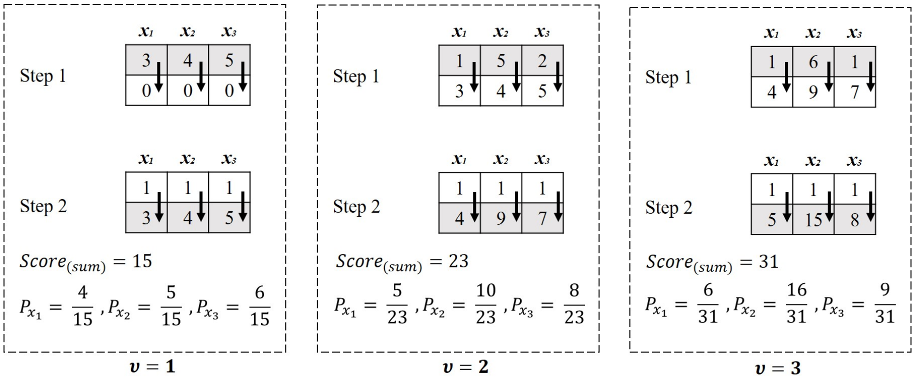

Fig. 5: An example illustrating the calculations of the application rates.

Fig. 5 shows an example of the CRM construction process, for three crossovers x_1 x_2, and x_3, with a cycle size $v = 3$. For every cycle, two steps are executed. First, scores are retrieved for each crossover. In this case, the first cycle has $Score_1 = 3$, $Score_2 = 4$ and $Score_3 = 5$. Next, the scores are shifted to $(2, i)$. Once a score is shifted to position $(2, i)$, a value of 1 is stored at position $(1, i)$, to ensure the application of all crossover functions, regardless of a crossover performance. If a crossover application has resulted in no improvement or even worse solution, it is still applied. The accumulated scores are then calculated by adding up the scores at the position $(1, i)$ to the scores at the position $(2, i)$. The active calculation of the application rates maintains a balance between the most effective operators, which provide good results, and week crossovers, which provide poor results.

5. Experimental Study and Results

Since parameter settings and running times stated in [5] were successful in providing good results, each run in the experiments here was executed with the same settings as shown in Table 5. Note that the crossover rate P_c and the mutation rate P_m values stated in Table 5 are used as initial settings for the AMCAGAs. However, these values are fixed when used with AMCGAs.

Similar to genetic operators rates, each WSRP problem set has different memory size σ. This value indicates the number of crossovers required to obtain enough information for the learning process, where $P_c \times \sigma = const$. Thus, the crossover rate P_c affects the value of σ, to record the crossover performances on at least $M/2$ of the population. For example, in smaller instances, $P_c = 50\%$, therefore, less crossovers are applied. Hence, larger σ is required to obtain sufficient information about the crossovers performances. In larger instances, $P_c = 100\%$, this means that more crossovers are applied, and a large memory size is not necessary.

Table 5: Parameter settings for AMCGAs and AMCAGA.

Parameter	**A**	**B**	**C**	**D**	**E**	**F**	Fixed	Initial Values
Mutation Rate P_m	50%	50%	30%	10%	10%	10%	AMCGAs	AMCAGAs
Crossover Rate P_c	50%	50%	50%	100%	100%	100%	AMCGAs	AMCAGAs
Population Size M	500	500	500	250	250	250	AMCGA, AMCAGA	-
Memory Size σ	250	250	250	125	125	125	AMCGA, AMCAGA	-

Different cycle settings were used here, where $\upsilon = \{5, 10, 15, 25, 40, 50\}$. These values were determined through preliminary experimentation. The testing revealed that a cycle of a size less than 5, had a slow learning process. A cycle of a size larger than 50 had a low accuracy of the learning factor, in which crucial information was lost. For example, a crossover operator might be the best performer at the start of a cycle, yet it can get worse in the same cycle.

Experimental results were grouped by the performance measurement method

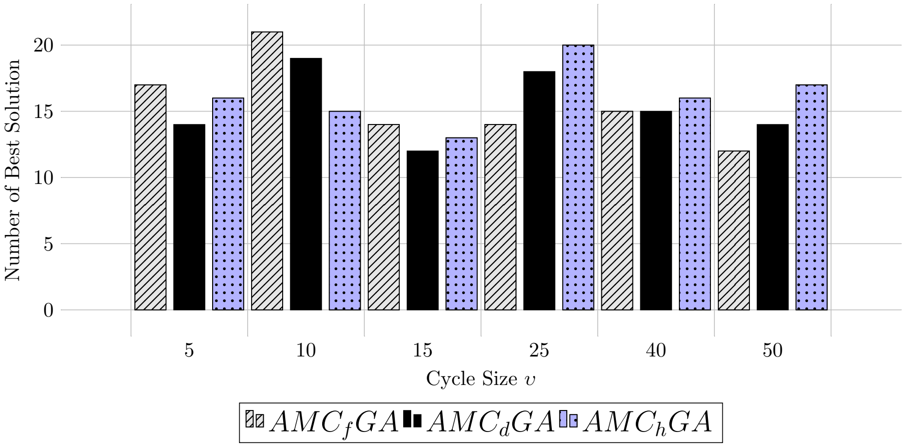

Fig. 6: Total number of best solutions produced by different rewarding mechanisms (AMC_fGA, AMC_dGA and AMC_hGA).

applied. Each measurement is noted as follows: fitness improvements (AMC_fGA), dissimilarities between individuals (AMC_dGA) and the hybrid approach (AMC_hGA). The best performing method was selected to be included in AMCAGA and combined with adaptive parameter control method AGA, presented in [6].

Each algorithm was executed 8 times (runs). This means that for each of the 42 problems instances, there were 8 × 6 (cycles) × 3 (methods) = 144 runs, seeded with the same initial population.

5.1. Performance of AMCGAs with Different Cycle Sizes

This set of experiments was conducted to investigate the effectiveness of the feedback mechanism in the AMCGAs, when using different cycle sizes. To do so, different cycle sizes were examined with respect to the method applied.

Fig. 6 shows the total number of best solutions for all problem instances. Each bar in the X-axis represents a rewarding method applied with a cycle of size υ. Methods shown in the plot are: AMC_fGA (grey bars with striped lines), AMC_dGA (black solid bars) and AMC_hGA (blue bars with dots). The higher the bar the better, i.e. the more ”best” values found.

It is clear that all methods provided relatively similar values with a slight increase on one of the methods over the others. Still, AMC_fGA obtained the highest number of best solutions. For AMC_fGA and AMC_dGA, the highest number of best solutions was the when $\upsilon = 10$. For AMC_hGA, on the other hand, the highest number of best solutions was when $\upsilon = 25$.

This result is related to scores given to an operator throughout the search, in which the accumulated score increases or decreases gradually. An operator performance at the start of the cycle might change drastically by the end of the cycle, especially when a large υ value is used. Nevertheless, $\upsilon > 25$ was proven to be less effective for all methods. Interestingly, the highest number of best solutions was obtained while using AMC_fGA, with $\upsilon = 10$. Hence, there is no need for larger υ value to keep long historical records.

With one performance measurement, i.e. AMC_fGA and AMC_dGA, small changes in the score values occur. This provided enough time for updating the application rate, for each crossover, and therefore these crossovers were used in the current population. On the other hand, a large υ was required when the hybrid performance measurement was applied. This is because of a large change in the score values that occurs as the outcome of combining both performance measurements. Nevertheless, if the υ was small, there was not enough time to reward all operators. Thus, one operator will dominate the algorithm, resulting in an uneven distribution of the application rates. Henceforth, a larger cycle-size was required. In summary, the larger the υ, the larger the increase in the score value.

Fig. 7 illustrates the overall average computational times in seconds, on problem sets A to F, for all methods. Each sub-figure corresponds to a cycle size υ and presents the average computational time used by AMC_fGA (grey bars with striped lines), AMC_dGA (black solid bars) and AMC_hGA (blue bars with dots). The lower the bar the better, i.e. the less computational time. On average, it was apparent from the plots that different methods provide solutions in approximately similar computational times.

For AMC_fGA, it was more computationally expensive to make large adjustments in the score values, especially when smaller υ was used. On the contrary, more time existed when using larger υ values, providing a shift in the score

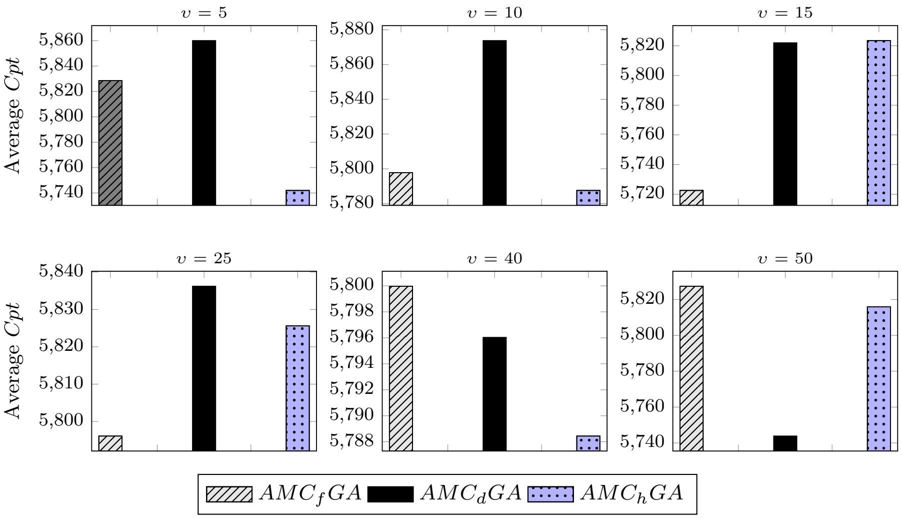

Fig. 7: Average computation-time (in seconds) produced by AMC variations with different cycle sizes υ.

values when AMC_fGA was used. Thus, the largest computational times for AMC_fGA, among all methods, was recorded when $\upsilon = 40$ or 50.

For AMC_dGA, more time was spent on calculating the scores, that resulted in more computational time, especially when υ was equal 5 to 25. This was the outcome of the diversity-based calculations, computed gene by gene, and executed V times for each individual to calculate the scores accurately.

Fitness-based calculations were faster than the diversity-based calculations. However, when υ was between 40 and 50, the sensitivity of the distance-based provided good solutions in less computational time. This is because that distance-based measurement method was more sensitive to the change of performances than fitness-based measurement. Note similar execution time to AMC_dGA with AMC_hGA was recorded, with $\upsilon = 15$.

Contrary to AMC_dGA, AMC_hGA was not affected by the convergence speed of the algorithm. The combinations between the diversity-based measurement and the fitness-based measurement in AMC_hGA have obtained better computational times than the separate methods. This is because AMC_hGA averaged the performances of both measurements by allowing the use of the calculations within the time limitations. The reason for this was the large increase in the score values due to both calculations. As a result, the scores were computed in less time while using AMC_hGA.

The next set of experiments was designed to use one cycle-size per method, selected according to the highest total number of best solutions (see Fig. 6). Thus, $\upsilon = 10$ was chosen for AMC_fGA as well as for AMC_dGA, and $\upsilon = 25$ was selected for AMC_hGA.

5.2. Overall Comparison Between AMCGAs methods

The second set of experiments was conducted to identify if there is a significant difference between the proposed AMCGAs variations or not. The work by [30] recommended the use of Friedman analysis as a non-parametric statistical test to establish statistical significance in EAs. Thus, a two-way Friedman analysis was used to measure the significant difference between groups of data when the dependent variable being measured was ordinal.

In this study, an IBM SPSS 22 two-way analysis was used to compare the variances of seven related-samples, with a significant level of $\alpha = 0.05$ and 95% as a confidence interval. Table 6 reports the results generated by the Friedman analysis on the 42 problem instances including the mean value, the standard deviation, the minimum cost-value, the maximum cost-value and the mean rank. The results presented in the mean rank column show the methods ranking based on the statistical analysis, where a low rank indicates the best method while a high rank indicates the worse method ranked overall. All problem instances were used to set the sample size of one method as large as possible, this increases the probability of accepting or rejecting the null hypothesis. Three additional values were calculated and used to measure the performance of each algorithm. **Dev** is the average percentage deviation from the best-known value (best solution of all the algorithms applied). **Best** is the fraction of instances in a set for which an algorithm matches the best-known value (best solution of all the algorithms applied). **Score** is the fraction of the instances for which a competing algorithm 'wins', i.e. produces better solutions than the configuration being scored. This score is calculated as $((q \times (p-1)) - r)/(q \times (p-1))$, where p is the number of methods compared, q is the number of problem instances, and r is the number of instances in which the $p-1$ competing configurations find a better result. Hence, the best score value is 1, when $r = 0$, and the worst score value is 0, when $r = q \times (p-1)$. The best results are highlighted in **bold**.

Table 6: Non-parametric Friedman's test results combined with performances metrics.

Method	Mean	Std. Deviation	Min	Max	Mean Rank	Dev %	# Best	Score
$\boldsymbol{AMC_fGA}$	287.07	699.78	1.18	3495.55	1.99	0.13%	0.50	0.65
$\boldsymbol{AMC_dGA}$	**286.74**	**699.11**	1.18	3496.73	**1.82**	**0.05%**	**0.64**	**0.73**
$\boldsymbol{AMC_hGA}$	287.23	700.10	1.18	3496.36	2.19	0.16%	0.33	0.46

Bold text refers to the best result.

We applied the Friedmann non-parametric statistical to the data in Table 6 and obtained a p-value of 0.02153 <0.05, degrees of freedom = 2 and $\chi^2 = 7.677$. This indicates the existence of significant performance differences among the three methods.

In order to examine where the differences actually occur, an additional analysis was implemented. Holm's test was chosen to detect the significance difference among all variations. The Holm procedure is an example of a step-down procedure. Step-up procedures start testing hypothesis H_m and step up through the sequence while retaining the hypotheses. The procedure stops at the first rejection (for example H_i), and $H_1, \ldots, H_i$ are all rejected.

In this case, Holm's method obtains the p-values higher than the significance level, that is to be interpreted in the sense that we do not have enough evidence to reject the null hypothesis.

However, the descriptive statistics and the measures explained above revealed that AMC_dGA method had the lowest mean value, standard deviation value, mean rank value and Dev% value. This method had also the highest fraction of the number of best solutions and the score values. This finding suggests that different methods applied to different datasets can obtain different results and henceforth each problem set benefited from each method accordingly.

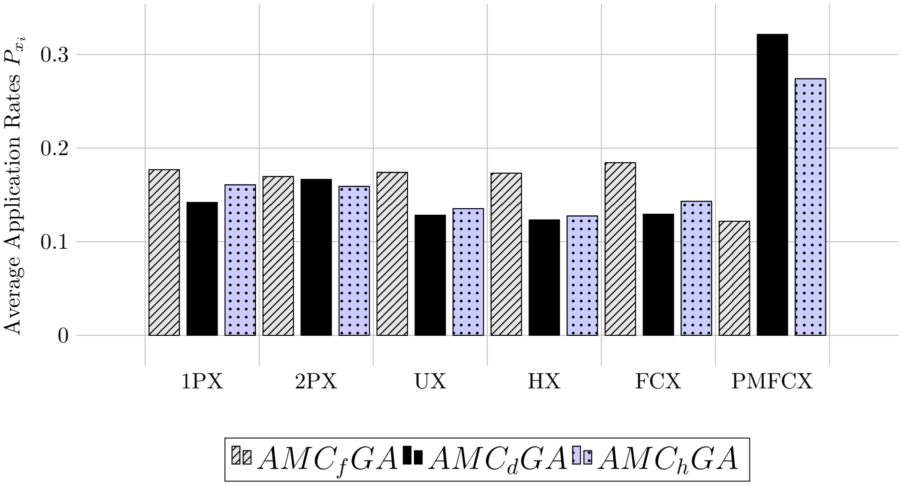

Fig. 8: Average application rates values used under different rewarding mechanisms (AMC_fGA, AMC_dGA, and AMC_hGA).

AMC_dGA obtained the best values in the above table. Thus, it can be argued that all variations were suitable for WSRP while AMC_dGA was slightly better than all the proposed multiple crossovers algorithms. Using the distance-based measurement has provided more accurate scores adjustments in comparison to other methods.

5.3. Crossovers Dominance Based on Application Rates Distribution

This section explores the change in the crossovers' application rates (P_{x_i}) to investigate the effectiveness of one crossover over the other, in each AMCGA. Thus, this set of experiments aims to identify the most used operator in each method applied, with respect to the performance measurement.

Each bar in the X-axis of Fig. 8 illustrates the average application rate P_{x_i} values, for all problem sets. All three methods were applied, with the set of crossovers, i.e. 1PX, 2PX, UX, HX, FCX and PMFCX. The AMC_fGA is plotted in grey bars with striped lines, the AMC_dGA is plotted as black solid bars and the AMC_hGA is plotted as blue bars with dots.

Among all crossovers applied with AMC_fGA, the values for the average P_{x_i} were relatively similar with a slight increase on FCX. This result further proves the observations stated in [5], that identified the FCX as one of the best

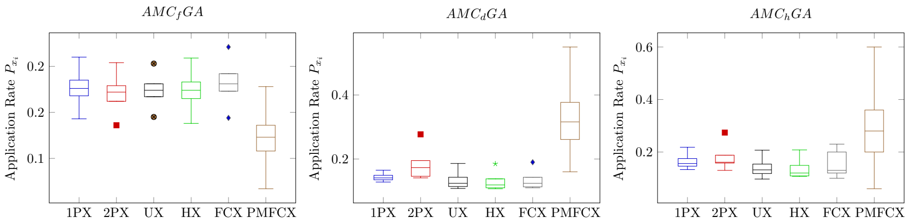

Fig. 9: Box plots comparing the average application rates for crossovers 1PX (blue), 2PX (red), UX (black), HX (green), FCX (grey) and PMFCX (brown).

crossovers for WSRP problem sets. Thus, this operator has been utilised more when a fitness-based performance measurement was utilised.

Nevertheless, the highest average application rate P_{x_i} among all crossovers was obtained by PMFCX, while using AMC_dGA. Hence, PMFCX was utilised more often when distance-based performance measurement was applied.

Faster calculations were required when using AMC_dGA and AMC_hGA. Thus, FCX was used less under these methods. On the other hand, the PMFCX crossover was utilised more, due to its fast calculations as a result of mixing heuristic approach with the traditional PMX crossover method.

Traditional crossovers have provided poor quality solutions that were comparatively similar to their parents. Still, using them alongside the problem-specific method can ensure various performances in the GA.

Fig. 9 shows a group of box plots to show overall patterns of response of change in application rates (P_{x_i}), for each crossover operator. Crossovers distribution corresponds to the current environment state if there is change in the P_{x_i} values, i.e the bigger the box plot the more diverse is the P_{x_i} values to the correspondent crossover.

Each sub-figure corresponds to the method applied, AMC_fGA, AMC_dGA and AMC_hGA. Each box-plot illustrates the average application rates (P_{x_i}) range, for each crossover and are shown in 1PX (blue), 2PX (red), UX (black), HX (green), FCX (grey) a PMFCX (brown).

As it can be seen from the plots, PMFCX box plot is lower than all other plots in AMC_fGA, i.e. less change in P_{x_i} values. The opposite occurs for AMC_dGA and AMC_hGA, where P_{x_i} values were more diverse. This indicates that PMFCX was updated more frequently. This result further supports the previous finding discussed in this section.

5.4. Effect of Using a Rewarding Process on AMCGA

The third set of experiments aims to compare AMCGA methods with an existing GA that was tailored for WSRP. The detailed results shown in Table 7 compares the indirect GA described in [5] (noted as GA) with the AMCGA variations (AMC_fGA, AMC_dGA and AMC_hGA). Crossovers used with indirect GA were specified for each problem set as follows. for A and B GCX, for C PMGreedyX, for D, E and F FCX. The FCF mutation was also used.

In addition to the indirect GA, the AMCGAs were compared against a variation of AMCGA that used a uniform choice of operators, noted as AMC_rGA. The goal is to investigate the performance of AMCGAs when excluding the reinforcement learning process. For each problem instance, the table shows the solution quality, noted as $f(S)$, and the computational time in seconds, noted as *Cpt*, in which the best solution was found.

Best values are highlighted in **bold**. If more than one method achieved the same result, among cost-best equals, the time-best is highlighted in **bold**.

As it can be seen from Table 7, the proposed methods AMC_fGA, AMC_dGA and AMC_hGA outperform the GA and AMC_rGA in terms of computational time, in particular AMC_fGA and AMC_dGA. This indicates that the rewarding process in the adaptive methods was more efficient time-wise. The percentage of best cost-values overall solutions are as follows. The GA 14.29%, AMC_rGA 30.95%, AMC_fGA 40.48%, AMC_dGA 47.48% and AMC_hGA 21.43%. Closer inspection of the results is discussed next.

Using a variety of operators, in which they have different performances, have provided good quality solutions for each problem set, especially AMC_fGA and AMC_dGA. Improvements have occurred due to the combined work of the operators, which allowed an extensive search with a larger variance than using one crossover. However, using two performance measurements, as the case in AMC_hGA was proven to be inefficient in comparison to the other AMCGAs.

Table 7: Results of the cost values $f(S)$ and computational time Cpt (in seconds) produced by the proposed methods GA, AMC_rGA, AMC_fGA, AMC_dGA and AMC_hGA for 42 WSRP instances.

		GA		AMC_rGA		AMC_fGA		AMC_dGA		AMC_hGA				GA		AMC_rGA		AMC_fGA		AMC_dGA		AMC_hGA	
		$f(S)$	Cpt	$f(S)$	Cpt	$f(S)$	Cpt	$f(S)$	Cpt	$f(S)$	Cpt			$f(S)$	Cpt	$f(S)$	Cpt	$f(S)$	Cpt	$f(S)$	Cpt	$f(S)$	Cpt
	1	3.49	34.08	3.49	3.90	3.49	2.27	3.49	1.85	**3.49**	**1.65**		**1**	173.15	2989.34	171.39	3140.40	171.08	3408.46	**170.71**	**3334.63**	171.08	3255.77
	2	2.96	396.77	2.49	5.07	2.54	2.34	2.49	2.62	**2.49**	**1.42**		**2**	169.56	3502.67	167.50	3448.17	168.11	3046.96	**167.31**	**3405.58**	168.31	3450.06
	3	3.65	436.92	3.01	153.54	**3.02**	**14.83**	3.02	58.57	3.02	115.48		**3**	184.49	3502.43	180.93	3211.17	180.86	3361.38	**180.86**	**3102.37**	181.55	3390.17
A	**4**	1.42	229.01	1.42	41.76	**1.42**	**41.54**	1.42	67.69	1.42	66.38	**D**	**4**	171.83	3484.81	168.68	3338.98	168.42	3323.28	168.37	3476.31	**167.86**	**3412.84**
	5	2.42	0.98	2.42	1.07	2.42	0.81	2.42	1.26	**2.42**	**0.42**		**5**	162.32	3589.68	161.93	3382.11	161.99	3266.39	**161.86**	**3276.84**	161.92	3113.17
	6	3.61	159.83	3.55	4.64	**3.55**	**3.21**	3.55	8.30	3.55	8.93		**6**	178.80	3446.80	178.16	3268.95	178.35	3209.79	**178.16**	**3353.26**	178.28	3278.63
	7	3.71	0.83	3.71	1.02	3.71	0.81	3.71	1.42	**3.71**	**0.32**		**7**	178.85	3423.81	178.65	3263.43	178.71	3367.56	178.65	3347.14	**178.59**	**3271.47**
	1	1.76	422.62	1.72	146.60	**1.72**	**141.90**	1.72	276.01	1.72	262.21		**1**	3.75	3314.33	1.18	3420.64	1.18	3366.72	1.18	3404.99	**1.18**	**3206.71**
	2	1.75	78.57	1.75	0.64	1.75	0.71	1.75	1.22	**1.75**	**0.34**		**2**	3.86	3570.60	1.21	3394.69	**1.21**	**3311.93**	1.21	3399.96	1.21	3431.21
	3	1.90	629.30	1.79	329.10	1.78	555.93	1.78	570.47	**1.78**	**435.03**		**3**	5.18	3371.76	1.22	3345.45	**1.21**	**3428.17**	1.22	3460.71	1.22	3395.24
B	**4**	2.08	29.51	2.08	4.77	**2.08**	**4.06**	2.08	21.25	2.08	7.28	**E**	**4**	3.27	3584.67	1.30	3419.12	1.29	3512.18	**1.29**	**3493.56**	1.30	3432.41
	5	1.96	434.63	1.91	417.83	**1.90**	**490.40**	1.91	483.60	1.92	558.09		**5**	5.15	3585.41	**2.24**	**3287.96**	2.24	3469.36	2.25	3424.19	2.25	3450.09
	6	1.71	343.74	1.64	105.39	1.65	80.54	**1.64**	**72.75**	1.65	137.81		**6**	3.56	3559.72	1.30	3406.16	**1.30**	**3233.54**	1.30	3356.92	1.30	3377.66
	7	1.87	502.96	1.80	248.04	**1.79**	**57.24**	1.80	244.68	1.79	144.08		**7**	3.92	3574.02	**1.73**	**3339.36**	1.73	3486.11	1.73	3452.58	1.73	3375.31
	1	115.13	846.87	115.01	597.34	114.81	513.89	**114.75**	**566.20**	114.88	641.68		**1**	2257.51	28710.28	2034.37	27834.65	2035.17	27760.40	**2022.40**	**28294.63**	2039.30	27768.47
	2	3.15	0.46	3.15	0.98	3.15	0.67	3.15	0.86	**3.15**	**0.20**		**2**	2306.05	28672.43	2084.22	27286.12	2084.84	27671.16	**2083.97**	**27978.79**	2084.47	27944.11
	3	104.83	657.11	105.02	659.60	**104.65**	**675.85**	104.89	434.64	104.82	535.76		**3**	850.24	28700.42	**608.07**	**27635.80**	608.32	27767.11	608.13	27867.36	608.63	27280.61
C	**4**	11.15	2.41	11.15	2.65	11.15	1.84	**11.15**	**1.79**	11.15	2.25	**F**	**4**	1546.96	28733.22	1329.08	26819.62	1328.77	27863.52	1329.58	28029.66	**1328.33**	**27308.04**
	5	12.34	3.38	12.34	16.09	12.34	2.94	12.34	68.90	**12.34**	**2.58**		**5**	453.99	28415.05	**196.57**	**26846.99**	197.57	26783.72	197.20	28222.74	198.51	28380.85
	6	180.98	591.22	180.98	367.50	**180.80**	**301.95**	180.80	431.25	180.86	377.21		**6**	855.31	28707.11	625.58	27613.17	624.96	27835.21	**624.96**	**27996.64**	625.77	27519.31
	7	**4.30**	**0.00**	**4.30**	**0.00**	4.30	0.00	4.30	0.00	4.30	0.00		**7**	3980.44	28660.10	3495.86	27970.66	**3495.55**	**28138.01**	3496.73	27705.17	3496.36	28333.90

Bold text refers to the best result.

This is due to the large jumps in the score values in comparison to using one performance measurement, i.e. AMC_fGA and AMC_dGA, where small movements into various directions in the solution space has resulted in finding undiscovered regions easier.

By contrast, in the indirect GA, the search was completed by one crossover involvement in a large proportion of the solution space. Using one crossover throughout the search has less ability to extend the search in those regions, which were most promising. This was the reason for the GA providing worse results than the AMCGAs.

On the other hand, random crossover selection has utilised different crossovers at an arbitrary level, without prior knowledge of the current search space. Still, the AMC_rGA has obtained the best results on E_5, E_7, F_3 and F_5. This was because of the lack of performance measurements calculations. Hence, results were computed faster under those instances.

In regard to computational time, AMCGAs proved to improve the efficiency of the algorithm by computing the results in less time. For GA, AMC_rGA, AMC_fGA, AMC_dGA and AMC_hGA, the average Cpt in seconds were 6069.04, 5756.7, 5797.7, 5873.8 and 5825.6 respectively. The reason for the rapid decrease in the computational times is as discussed next.

In the traditional GA, one crossover was applied at each iteration. As a result, the algorithm required more time to improve the solution. On the other hand, the AMCGAs enforce the performances of different crossovers onto one population, which was made in a minimum time. Therefore, the proposed AMCGAs obtain solutions in fewer iterations than the indirect GA. In AMC_rGA, the average Cpt was the lowest among all compared methods, this was due to the exclusion of the feedback process. The average Cpt for AMC_fGA was less than the average Cpt for AMC_dGA and AMC_hGA. This result was the outcome of computing the dissimilarities between the parent and the offspring, which resulted in a massive amount of calculations. Despite the fact that in AMC_hGA the two performance measurements were applied, it obtained the results in less Cpt-time than AMC_dGA. This outcome was due to the use of

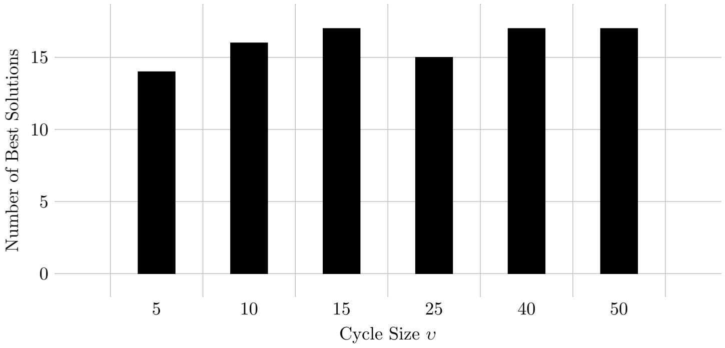

Fig. 10: Total number of best solutions while using AMC_dAGA.

the rewarding process that resulted in better and faster convergence.

5.5. *Using an AMC_dGA as a Component of AMCAGA*

A major advantage of AMCGAs was that they have a considerable influence on improving the efficiency of the baseline GA, especially when the distance-based performance measurement was applied. Thus, the AMC_dGA method was selected to be integrated with the adaptive operator rates control method AMCAGA (noted as AMC_dAGA), that perform as a full adaptive GA. The following experiments aimed to evaluate the validity of AMC_dAGA by providing further insights into its performance.

5.5.1. *Effect of Uing Different Cycle Sizes in AMCAGA*

In this section, the aim was to investigate the effect of the using different cycle sizes in AMC_dAGA on solutions quality and computational times.

Fig. 10 shows the total number of best solutions generated by different cycle sizes. Each bar at the X-axis represents an AMC_dAGA method applied with a cycle size υ. The higher the bar the better, i.e. the more "best" values. Using different cycle sizes has resulted in relatively similar performance, with a high number of best solutions in more than one cycle size. Thus, it can be claimed that using adaptive operator rates (P_c and P_m) makes the performance of the AMCGA more stable than using the AMC_dGA separately, as seen on Fig. 6 and Fig. 10.

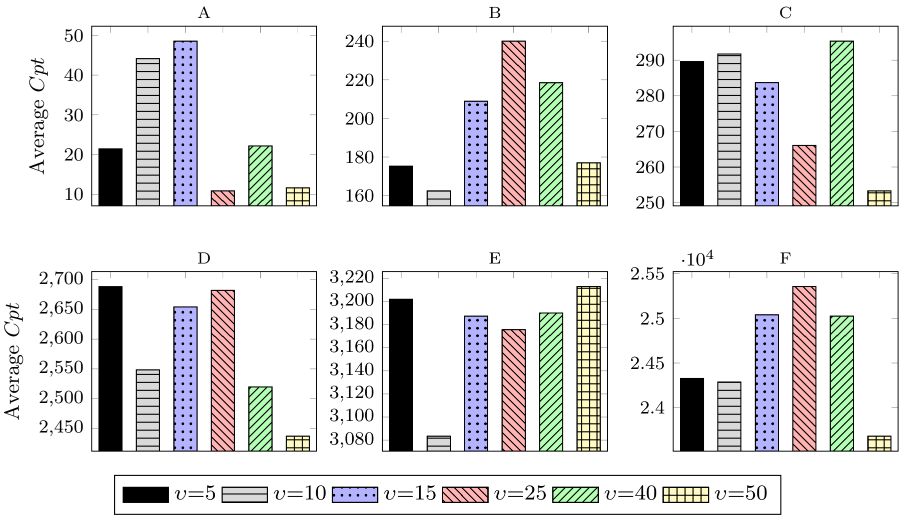

Fig. 11: Average computational-time (in seconds) produced by AMC_dAGA used with different cycle sizes υ.

The number of best solutions was the highest when $\upsilon = 15$, 40 and 50 with a value of 17 best solutions. Followed by $\upsilon = 10$ with 16 solutions and $\upsilon = 25$ with 15 solutions. The values for the number of best solutions when $\upsilon = 5$ was the lowest. The time was insufficient to score all operators. Thus, a large cycle size, i.e. 50, provides better learning outcomes with the time to retrieve the information needed in order to improve the results.

Another observation was made when recording the computational times for AMC_dAGA while using different cycle sizes. Each sub-figure in Fig. 11 corresponds to a problem sets from A to F, and each bar illustrates the overall average of the computational time in seconds used by a cycle-size. The bars colour and pattern indicate each cycle as follows: black solid bars when cycle size = 5, grey bars with stripped lines when $\upsilon = 10$, blue bars with dots when $\upsilon = 15$, red bars with right inclined lines when $\upsilon = 25$, green bars with left inclined lines when $\upsilon = 40$ and yellow bars with a grid when $\upsilon = 50$. The lower the bar the better, i.e. the less computational time.

On average, the lowest computational times for problem set A was when $\upsilon = 25$, however, all cycle sizes have obtained the same result in less than 50 seconds which was acceptable. Followed by the $\upsilon = 50$ that also obtained the lowest average computational times for problem sets C, D and F. The results, as shown in Figures 11 and 10, indicate that combining the adaptive operator rates (P_c and P_m) approach with AMC_dGA of a cycle of size 50 provides the best results in less time, especially for difficult problem sets. The larger the cycle size, the more scores were calculated for an operator effectiveness in addition to updating the operator rates. As a result, the population evolved over time into better, fitter solutions. The interchange between the two adaptive aspects was vastly exploited in AMC_dAGA. Note that the lowest average computational times for problem sets B and E were when $\upsilon = 10$ with a difference between 100 to 200 seconds to the other sizes. With reference to Fig. 10, this cycle size also obtained the second highest number of best solutions. Therefore, the results for a $\upsilon = 10$ and $\upsilon = 50$ is investigated further in the next section.

5.5.2. Overall Results of AMCAGA vs. AMCGA and AGA

The aim of this experiments is to compare the performance of AMC_dAGA against AMC_dGA and AGA to understand the effect of combining the adaptive parameter mechanisms into the AMCs.

Results for AMC_dAGA are shown in Table 8 with the diversity-based adaptive operators rate control GA (noted as AGA) and the AMCGA variations that utilised diversity-based measurement (noted as AMC_dGA). The AMC_dAGA method used in this comparison was when $\upsilon = 10$ (noted as AMC_dAGA_{10}) and a $\upsilon = 50$ (noted as AMC_dAGA_{50}). These methods are selected based on the observations form Fig. 6 and Fig. 7.

Note that there are two types of adaptability in Table 8. The first adaptive method used in AGA and AMC_dAGA is the GA parameter control, P_c and P_m, The second adaptive method used in AMC_dGA and AMC_dAGA is multiple crossover adaptability. The baseline GA was excluded in this comparison because it was shown that AMC_dGA and AGA provided better results as discussed earlier.

From the table, it can be seen that AMC_dAGA outperformed AGA and

Table 8: Results comparison between cost values $f(S)$ and computational time Cpt (in seconds) produced by the adaptive methods AGA, AMC_dGA, AMC_dAGA_{10} and AMC_dAGA_{50} for 42 WSRP instances.

		AGA		AMC_dGA		AMC_dAGA_{10}		AMC_dAGA_{50}				AGA		AMC_dGA		AMC_dAGA_{10}		AMC_dAGA_{50}	
		f(S)	*Cpt*	*f (S)*	*Cpt*	*f (S)*	*Cpt*	*f (S)*	*Cpt*			*f(S)*	*Cpt*	*f (S)*	*Cpt*	*f (S)*	*Cpt*	*f (S)*	*Cpt*
A	**1**	3.49	14.45	3.49	1.85	3.49	2.81	**3.49**	**1.78**	**D**	**1**	170.77	2978.51	170.71	3334.63	**170.23**	**2533.55**	170.29	2545.39
	2	2.49	100.69	2.49	2.62	2.49	4.49	**2.49**	**1.27**		**2**	166.87	3228.52	167.31	3405.58	166.58	2109.05	**166.26**	**2512.36**
	3	3.08	11.50	3.02	58.57	3.02	221.92	**3.02**	**27.63**		**3**	180.60	3258.30	180.86	3102.37	179.81	2490.46	**179.75**	**2370.22**
	4	1.42	247.07	1.42	67.69	1.42	51.27	**1.42**	**42.71**		**4**	167.93	3465.12	168.37	3476.31	166.64	2382.08	**166.39**	**2511.47**
	5	2.42	1.11	2.42	1.26	2.42	0.87	**2.42**	**0.38**		**5**	161.73	3367.04	161.86	3276.84	161.50	2503.26	**161.37**	**2532.9**
	6	3.56	130.22	3.55	8.30	3.55	26.59	**3.55**	**7.05**		**6**	178.28	3200.96	178.16	3353.26	178.11	2765.96	**177.99**	**2368.7**
	7	3.71	0.72	3.71	1.42	3.71	1.03	**3.71**	**0.51**		**7**	**178.40**	**2489.11**	178.65	3347.14	178.41	3054.21	178.41	2217.13
B	**1**	1.75	84.00	1.72	276.01	**1.72**	**160.06**	1.73	146.45	**E**	**1**	1.18	3322.13	1.18	3404.99	1.17	3390.71	**1.17**	**3285.83**
	2	1.75	0.56	1.75	1.22	1.75	1.03	**1.75**	**0.29**		**2**	1.21	3368.60	1.21	3399.96	**1.20**	**3303.48**	1.20	3311.01
	3	1.82	280.35	1.78	570.47	**1.77**	**327.03**	1.79	468.52		**3**	1.21	3246.99	1.22	3460.71	1.21	3181.93	**1.21**	**3137.97**
	4	2.08	46.19	2.08	21.25	2.08	5.12	**2.08**	**3.17**		**4**	1.29	3492.21	1.29	3493.56	**1.29**	**2932.00**	1.29	3123.67
	5	1.93	98.85	1.91	483.60	1.92	459.26	**1.91**	**396.11**		**5**	2.24	3442.02	2.25	3424.19	**2.24**	**2921.37**	2.24	3378.24
	6	1.66	190.74	**1.64**	**72.75**	1.65	97.23	1.64	146.05		**6**	1.30	3283.59	1.30	3356.92	**1.30**	**2539.72**	1.30	2975.27
	7	1.81	154.78	1.80	244.68	1.80	87.54	**1.80**	**78.43**		**7**	1.73	3473.85	1.73	3452.58	1.72	3314.44	**1.72**	**3278.99**
C	**1**	115.07	703.71	**114.75**	**566.20**	114.87	644.23	114.94	640.35	**F**	**1**	2122.60	27647.63	2022.40	28294.63	2036.82	23117.21	**2019.72**	**22709.3**
	2	3.15	0.46	3.15	0.86	3.15	0.71	**3.15**	**0.30**		**2**	2082.79	26318.27	2083.97	27978.79	2081.99	23765.59	**2081.74**	**22516.9**
	3	105.08	677.45	104.89	434.64	104.75	804.69	**104.82**	**681.10**		**3**	607.26	27722.40	608.13	27867.36	605.14	22220.34	**604.71**	**22658.5**
	4	11.15	2.40	**11.15**	**1.79**	11.15	3.14	11.15	2.64		**4**	1328.51	27229.31	1329.58	28029.66	1326.28	24782.11	**1325.90**	**23459**
	5	12.60	33.70	12.34	68.90	12.34	2.40	**12.34**	**2.35**		**5**	196.08	26934.63	197.20	28222.74	193.59	25631.57	**192.78**	**25895.8**
	6	180.99	589.30	**180.80**	**431.25**	180.92	586.95	180.99	446.39		**6**	624.77	25367.39	624.96	27996.64	622.41	26415.45	**622.34**	**23680**
	7	**4.30**	**0.00**	**4.30**	**0.00**	**4.30**	**0.00**	**4.30**	**0.00**		**7**	3495.99	27225.77	3496.73	27705.17	**3492.87**	**24083.07**	3493.18	24846.2

Bold text refers to the best result.

AMC_dGA, especially AMC_dAGA_{50}. Closer inspection of the results shows the percentage of best cost-values overall solutions are as follows. The AGA 21.43%, AMC_dGA 35.71%, AMC_dAGA_{10} 42.86% and AMC_dAGA_{50} 59.52%. Hence, AMC_dAGA_{50} has provided the best results on 59.52% of all solutions. Followed by AMC_dAGA_{10} that provided the best results on 42.86% of all solutions. These results indicate the power of combining two adaptive elements that work together in order to improve the GA offspring productivity.

Another advantage of this method was the rapid decrease in computational time that was previously reduced by using the adaptive methods separately in comparison to the baseline GA. The average computational times in seconds were 5653.11, 5873.79, 5069.67 and 4962.10 for AGA, AMC_dGA, AMC_dAGA_{10} and AMC_dAGA_{50} respectively. Thus, using the combined method was more cost-effective than using one method individually for WSRP.

5.6. Results of AMCAGA vs. WSRPs Solution Methods

This section provides a comparison of the best-performing methods proposed in this study, i.e., AMC_dAGA_{10} and AMC_dAGA_{50}, against three existing WSRP solution methods from the literature: MIP solver [7], MIP with decomposition [31] and VNS algorithm [8]. Table 9 shows the solution quality, noted as $f(S)$, and the computational time in seconds, noted as *Cpt*, in which the best solution was found. The best values are highlighted in **bold**.

For smaller problem sets, the proposed methods were quite competitive, matching the best-known results for many of those instances. The VNS seems to provide better overall results with 42.86% of all best solutions. However, the AMC_dAGA_{10} and AMC_dAGA_{50} outperformed the MIP with decomposition method with 21.43% and 42.86% of all best solutions respectively.

The average computational times were calculated for methods that provided solutions for all instances. i.e. MIP with decomposition AMC_dAGA_10 and AMC_dAGA_50. The recorded times were 4964.26, 5069.67 and 4962.10 respectively.

The AMC_dAGA_{10} has the largest computational time among all methods.

Table 9: Cost-values $f(S)$ and computational-time Cpt (in seconds) for WSRP instances, produced by all WSRP solution methods on 42 instances.

		Optimal		MIP DECOMP.		VNS		AMC_dAGA_{10}		AMC_dAGA_{50}				Optimal		MIP DECOMP.		VNS		AMC_dAGA_{10}		AMC_dAGA_{50}	
		f (S)	*Cpt*	*f (S)*	*Cpt*	*f (S)*	*Cpt*	*f(S)*	*Cpt*	*f(S)*	*Cptn*			*f (S)*	*Cpt*	*f (S)*	*Cpt*	*f (S)*	*Cpt*	*f(S)*	*Cpt*	*f(S)*	*Cptn*
A	**01**	3.49	7.00	5.65	3.71	3.49	2.99	3.49	2.81	**3.49**	**1.78**	**D**	**01**	**n/a**	**n/a**	496.4	1060.0	**170.3**	**3036.2**	170.23	2533.55	170.29	2545.39
	02	2.49	8.00	4.53	3.58	**2.49**	**0.33**	2.49	4.49	2.49	1.27		**02**	**n/a**	**n/a**	372.9	1192.1	**163.9**	**2840.8**	166.58	2109.05	166.26	2512.36
	03	**3.00**	**14.00**	10.65	3.70	3.00	29.30	3.02	221.92	3.02	27.63		**03**	**n/a**	**n/a**	3213.3	1209.0	**178.2**	**3172.8**	179.81	2490.46	179.75	2370.22
	04	**1.42**	**5.00**	3.09	2.88	1.42	6.87	1.42	51.27	1.42	42.71		**04**	**n/a**	**n/a**	418.9	3005.1	167.1	3313.8	166.64	2382.08	**166.39**	**2511.47**
	05	2.42	1.00	3.54	1.77	**2.42**	**0.11**	2.42	0.87	2.42	0.38		**05**	**n/a**	**n/a**	243.9	1306.7	**161.1**	**2818.5**	161.50	2503.26	161.37	2532.90
	06	3.55	5.00	3.74	2.42	3.55	29.47	3.55	26.59	**3.55**	**7.05**		**06**	**n/a**	**n/a**	1411.3	1222.0	**177.4**	**2996.0**	178.11	2765.96	177.99	2368.70
	07	3.71	1.00	4.81	1.64	**3.71**	**0.07**	3.71	1.03	3.71	0.51		**07**	**n/a**	**n/a**	753.3	1361.9	177.9	2930.4	178.41	3054.21	**178.41**	**2217.13**
B	**01**	**1.70**	**21.00**	1.79	8.07	1.70	156.45	1.72	160.06	1.73	146.45	**E**	**01**	**n/a**	**n/a**	33.0	8408.0	**n/a**	**n/a**	1.17	3390.71	**1.17**	**3285.834**
	02	1.75	2.00	1.89	4.29	**1.75**	**0.00**	1.75	1.03	1.75	0.29		**02**	**n/a**	**n/a**	26.0	12448.4	**n/a**	**n/a**	**1.20**	**3303.48**	1.20	3311.008
	03	1.72	6003.00	2.06	32.86	**1.72**	**473.21**	1.77	327.03	1.79	468.52		**03**	**n/a**	**n/a**	29.0	20746.6	**n/a**	**n/a**	1.21	3181.93	**1.21**	**3137.972**
	04	2.07	25.00	2.21	15.25	**2.07**	**9.03**	2.08	5.12	2.08	3.17		**04**	**n/a**	**n/a**	28.5	15190.5	**n/a**	**n/a**	**1.29**	**2932.00**	1.29	3123.67
	05	**1.82**	**585.00**	4.74	25.35	1.83	135.33	1.92	459.26	1.91	396.11		**05**	**n/a**	**n/a**	270.1	32619.2	**n/a**	**n/a**	**2.24**	**2921.37**	2.24	3378.24
	06	**1.62**	**184.00**	2.52	24.11	1.62	194.29	1.65	97.23	1.64	146.05		**06**	**n/a**	**n/a**	24.6	24212.1	**n/a**	**n/a**	**1.30**	**2539.72**	1.30	2975.266
	07	**1.79**	**300.00**	4.06	23.64	1.79	304.96	1.80	87.54	1.80	78.43		**07**	**n/a**	**n/a**	427.8	51057.3	**n/a**	**n/a**	1.72	3314.44	**1.72**	**3278.994**
C	**01**	**n/a**	**n/a**	904.98	211.64	**114.21**	**301.32**	114.87	644.23	114.94	640.35	**F**	**01**	**n/a**	**n/a**	64305.1	3446.4	**n/a**	**n/a**	2036.82	23117.21	**2019.72**	**22709.26**
	02	3.15	6.00	3.61	0.57	**3.15**	**0.00**	3.15	0.71	3.15	0.30		**02**	**n/a**	**n/a**	73291.2	1111.0	**n/a**	**n/a**	2081.99	23765.59	**2081.74**	**22516.85**
	03	**n/a**	**n/a**	1186.27	26.33	**103.52**	**550.29**	104.75	804.69	104.82	681.10		**03**	**n/a**	**n/a**	115235.2	4555.1	**n/a**	**n/a**	605.14	22220.34	**604.71**	**22658.5**
	04	11.15	90.00	81.25	3.09	**11.15**	**0.91**	11.15	3.14	11.15	2.64		**04**	**n/a**	**n/a**	102994.2	4219.2	**n/a**	**n/a**	1326.28	24782.11	**1325.90**	**23458.95**
	05	12.34	55.00	68.94	1.05	**12.34**	**0.34**	12.34	2.40	12.34	2.35		**05**	**n/a**	**n/a**	101438.2	6156.5	**n/a**	**n/a**	193.59	25631.57	**192.78**	**25895.77**
	06	**n/a**	**n/a**	3102.26	47.05	**140.44**	**323.52**	180.92	586.95	180.99	446.39		**06**	**n/a**	**n/a**	76007.1	9695.6	**n/a**	**n/a**	622.41	26415.45	**622.34**	**23680.04**
	07	4.30	1.00	5.29	0.24	4.30	0.02	**4.30**	**0.00**	**4.30**	**0.00**		**07**	**n/a**	**n/a**	176540.6	3832.8	**n/a**	**n/a**	**3492.87**	**24083.07**	3493.18	24846.23

Bold text refers to the best result.

On the contrary, the AMC_dAGA_{50} has the lowest computation time among all methods. These findings indicate that the use of a large cycle size provided better GA performance, especially cost-wise. A noticeable effect of using adaptive aspects was the reduction of the computation time, which was also enhanced when using AMCAGA. On the other hand, the MIP with decomposition method has obtained a low average computation time. However, the results obtained were poor in comparison to the other methods.

So far, the proposed methods were the only algorithms that provided results for all instances. Hence, these adaptive GAs were able to solve this real-world and highly constrained optimisation problem instances. Interestingly, the best cost values were obtained by diversity-based methods. This further proves the significance of maintaining a diverse population in enhancing the GA performance when tackling WSRP. Even though VNS had obtained better results than the proposed methods in this study, when results were available, this study helps to better understand the applicability of GAs for WSRP.

6. Conclusion

Using synergies between genetic operators can provide better results than using one operator during the search [20]. This concept is used in this study by proposing an Adaptive Multiple Crossover Genetic Algorithm (AMCAGA) to tackle 42 instances of a Workforce Scheduling and Routing Problem (WSRP) in Home Healthcare.

Six different crossover operators are used within the proposed AMCAGA method. An adaptive mechanism seeks to learn the best way to apply the crossovers by rewarding their effectiveness in the current stage of the search. Three performance measurements are used to evaluate a crossover. One based on fitness, another one based on Hamming distance and the third one being a hybrid of the first two. Variations of the algorithm (AMC_fGA, AMC_dGA, AMC_hGA) using these performance measurements were tested and experimental results indicated that the Hamming distance variant (AMC_dGA) produced the best results although it was also the most time consuming.

Experiments were executed to compare the performance of the proposed AMCAGA with several other methods including MIP with decomposition [31], VNS algorithm [8], indirect GA (non-adaptive) [5], randomly uniform variant AMC_rGA (with no learning) and adaptive parameter control GA (AGA) [6]. Overall, the proposed method exhibited better performance particualrly in respect of diversity. The adaptive learning scheme to manage the multiple crossovers has effectively improved the GA's performance on the WSRP considered here. The adaptive learning scheme includes mechanisms for controlling crossover and mutation rates (P_c and P_m probabilities) of multiple crossovers resulting in better quality solutions in less computational time. This paper has contributed to better understanding of how to effectively apply GAs to this difficult and highly-constrained optimisation problem that combines scheduling and routing.

Future work is required to investigate whether the proposed solution method would also perform well on other WSRP scenarios like technician scheduling and similar problems involving a mobile workforce performing tasks on different locations. This type of problems incorporating scheduling and routing are fertile ground for investigating the effective design of evolutionary algorithms and this paper has sought to make a contribution in this regard.

References

[1] R. Lassaigne, M. De Rougemont, Logic and complexity, Springer Science & Business Media, 2012.

[2] P. Cowling, N. Colledge, K. Dahal, S. Remde, The trade-off between diversity and quality for multi-objective workforce scheduling, in: Proceedings of the 6th European Conference on Evolutionary Computation in Combinatorial Optimization, EvoCOP'06, Springer-Verlag, Berlin, Heidelberg, 2006, pp. 13–24.

[3] M. Mutingi, C. Mbohwa, Health-care staff scheduling in a fuzzy environment: A fuzzy genetic algorithm approach, in: Conference Proceedings (DFC Quality and Operations Management), International Conference on Industrial Engineering and Operations Management, 2014, pp. 303–312.

[4] H. ALgethami, D. Landa-Silva, A. Martinez-Gavara, Selecting genetic operators to maximise preference satisfaction in workforce scheduling and routing problem, in: Proceedings of the 6th International Conference on Operations Research and Enterprise Systems (ICORES)., Porto, Portugal, 2017, pp. 416–423.

[5] H. Algethami, R. L. Pinheiro, D. Landa-Silva, A genetic algorithm for a workforce scheduling and routing problem, in: 2016 IEEE Congress on Evolutionary Computation (CEC), 2016, pp. 927–934.

[6] H. Algethami, D. Landa-Silva, Diversity-based adaptive genetic algorithm for a workforce scheduling and routing problem, in: 2017 IEEE Congress on Evolutionary Computation (CEC), 2017, pp. 1771–1778.

[7] W. Laesanklang, D. Landa-Silva, Decomposition techniques with mixed integer programming and heuristics for home healthcare planning, Annals of Operations Research (2016) 1–35.

[8] R. L. Pinheiro, D. Landa-Silva, J. Atkin, A variable neighbourhood search for the workforce scheduling and routing problem, in: Advances in Nature and Biologically Inspired Computing, Springer, Pietermaritzburg, South Africa, 2016, pp. 247–259.

[9] J. Maturana, F. Saubion, A compass to guide genetic algorithms, in: G. Rudolph, T. Jansen, N. Beume, S. Lucas, C. Poloni (Eds.), Parallel Problem Solving from Nature – PPSN X: 10th International Conference, Dortmund, Germany, September 13-17, 2008. Proceedings, Springer Berlin Heidelberg, Berlin, Heidelberg, 2008, pp. 256–265.

[10] P. Consoli, X. Yao, Diversity-driven selection of multiple crossover operators for the capacitated arc routing problem, in: C. Blum, G. Ochoa (Eds.), Evolutionary Computation in Combinatorial Optimisation: 14th European Conference, EvoCOP 2014, Granada, Spain, April 23-25, Revised Selected Papers, Springer Berlin Heidelberg, Berlin, Heidelberg, 2014, pp. 97–108.

[11] C. Contreras-Bolton, G. Gatica, C. R. Barra, V. Parada, A multi-operator genetic algorithm for the generalized minimum spanning tree problem, Expert Systems with Applications 50 (2016) 1 – 8.

[12] K. Puljić, R. Manger, Comparison of eight evolutionary crossover operators for the vehicle routing problem, Mathematical Communications 18 (2) (2013) 359–375.

[13] E. Osaba, E. Onieva, R. Carballedo, F. Diaz, A. Perallos, An adaptive multi-crossover population algorithm for solving routing problems, in: Nature Inspired Cooperative Strategies for Optimization (NICSO 2013), Springer, 2014, pp. 113–124.

[14] J. Belluz, M. Gaudesi, G. Squillero, A. Tonda, Operator selection using improved dynamic multi-armed bandit, in: Proceedings of the 2015 Annual Conference on Genetic and Evolutionary Computation, GECCO '15, ACM, New York, NY, USA, 2015, pp. 1311–1317.

[15] W. M. Spears, Adapting crossover in evolutionary algorithms, in: Proceedings of the Fourth Annual Conference on Evolutionary Programming, MIT Press, 1995, pp. 367–384.

[16] A. L. Tuson, Adapting operator probabilities in genetic algorithms, Tech. rep., Master's thesis, Evolutionary Computation Group, Dept. of Artificial Intelligence, Edinburgh University (1995).

[17] D. Thierens, An adaptive pursuit strategy for allocating operator probabilities, in: Proceedings of the 7th Annual Conference on Genetic and Evolu-

tionary Computation, GECCO '05, ACM, New York, NY, USA, 2005, pp. 1539–1546.

[18] P. Auer, N. Cesa-Bianchi, P. Fischer, Finite-time analysis of the multiarmed bandit problem, Machine Learning 47 (2) (2002) 235–256.

[19] Á. Fialho, L. Da Costa, M. Schoenauer, M. Sebag, Analyzing bandit-based adaptive operator selection mechanisms, Annals of Mathematics and Artificial Intelligence 60 (1) (2010) 25–64.

[20] K. Li, . Fialho, S. Kwong, Q. Zhang, Adaptive operator selection with bandits for a multiobjective evolutionary algorithm based on decomposition, IEEE Transactions on Evolutionary Computation 18 (1) (2014) 114–130.

[21] D. Mankowska, F. Meisel, C. Bierwirth, The home health care routing and scheduling problem with interdependent services, Health Care Management Science 17 (1) (2014) 15–30.

[22] M. S. Rasmussen, T. Justesen, A. Dohn, J. Larsen, The home care crew scheduling problem: Preference-based visit clustering and temporal dependencies, European Journal of Operational Research 219 (3) (2012) 598 – 610.

[23] J. A. Castillo-Salazar, D. Landa-Silva, R. Qu, Workforce scheduling and routing problems: literature survey and computational study, Annals of Operations Research 239 (1) (2016) 39–67.

[24] M. Misir, P. Smet, K. Verbeeck, G. Vanden Berghe, Security personnel routing and rostering: A hyper-heuristic approach, in: Proceedings of the 3rd International Conference on Applied Operational Research, Vol. 3, Tadbir, 2011, pp. 193–205.

[25] S. Hartmann, A competitive genetic algorithm for resource-constrained project scheduling, Naval Research Logistics (NRL) 45 (7) (1998) 733–750.

[26] P. C. Chu, J. E. Beasley, A genetic algorithm for the multidimensional knapsack problem, Journal of heuristics 42 (1) (1998) 63–86.

[27] M. Črepinšek, S.-H. Liu, M. Mernik, Exploration and exploitation in evolutionary algorithms: A survey, ACM Comput. Surv. 45 (3) (2013) 35:1–35:33.

[28] R. W. Morrison, K. A. De Jong, Measurement of population diversity, in: Artificial Evolution: 5th International Conference, Evolution Artificielle, EA 2001 Le Creusot, France, October 29–31, 2001 Selected Papers, Springer Berlin Heidelberg, Berlin, Heidelberg, 2002, pp. 31–41.

[29] J. M. Whitacre, T. Q. Pham, R. A. Sarker, Use of statistical outlier detection method in adaptive evolutionary algorithms, in: Proceedings of the 8th Annual Conference on Genetic and Evolutionary Computation, GECCO '06, ACM, New York, NY, USA, 2006, pp. 1345–1352.

[30] S. García, D. Molina, M. Lozano, F. Herrera, A study on the use of non-parametric tests for analyzing the evolutionary algorithms' behaviour: a case study on the cec'2005 special session on real parameter optimization, Journal of Heuristics 15 (6) (2008) 617.

[31] W. Laesanklang, R. Lankaites-Pinheiro, H. Algethami, D. Landa-Silva, Extended decomposition for mixed integer programming to solve a workforce scheduling and routing problem, in: D. de Werra, G. H. Parlier, B. Vitoriano (Eds.), Operations Research and Enterprise Systems: 4th International Conference, ICORES 2015: revised selected papers, Vol. 577 of Communications in Computer and Information Science, Springer International Publishing, Lisbon, Portugal, 2015, pp. 191–211.